ORIGINAL PAPER

A.V.C. Sobral · W. Ristow Jr.
S.C. Domenech · C.V. Franco

Characterization and corrosion behavior of injection molded 17-4 PH steel electrochemically coated with poly[*trans*-dichloro(4-vinylpyridine)ruthenium]

Abstract The present study describes preliminary results on the corrosion resistance of injection molded 17-4 PH stainless steel potentiostatically coated with poly{*trans*-[RuCl$_2$(vpy)$_4$]}, where vpy (4-vinylpyridine) acts as a ligand. The coated electrodes were characterized by scanning electron microscopy and energy dispersive spectroscopy, as well as by electrochemical techniques. The microstructural analysis indicated that the films reached up to 100 μm thickness. Cyclic voltammetry was carried out in 0.1 M tetrabutylammonium hexafluorophosphate/methyl isobutyl ketone. The results revealed a scan rate dependent wave corresponding to a Ru^{2+}/Ru^{3+} redox reaction, thus confirming the presence of ruthenium in the films. Anodic polarization tests were performed in 3% NaCl in order to estimate the anodic dissolution current density and the corrosion rate of the material. The results indicated that coating the substrate improved the corrosion resistance of the material.

Key words Electropolymerization · Protective coating · Corrosion · Injection molding

Introduction

The use of electrochemically polymerized monomers has been extensively studied in order to improve the corrosion resistance of sintered steel parts. A new approach to the problem, involving the deposition of electroactive polymeric films, has attracted the interest of different research groups [1, 2]. We report the study of a new class of polymerized monomers to coat metallic surfaces, including poly{*trans*-[RuCl$_2$(pmp)$_4$]} (pmp = 3-(pyrrole-1-

A.V.C. Sobral · S.C. Domenech · C.V. Franco (✉)
LEC Departamento de Química,
UFSC Campus Trindade CFM,
88040-900 Florianópolis-SC, Brazil

W. Ristow Jr.
Lupatech S/A, Divisão Steelinject, Caixa Postal 1215,
Distrito Industrial, 95112-090 Caxias do Sul-RS, Brazil

ylmethyl)pyridine) [3–5] and poly{*trans*-[RuCl$_2$(vpy)$_4$]} (vpy = 4-vinylpyridine) [6]. Steel surfaces have been successfully coated by the latter, as a consequence of the use of vpy as a ligand. The use of such compounds prevents the dissolution of alloying elements upon electrocoating, as the ligand can be reductively polymerized. Complexes containing vinylpyridine (as well as vinylbipyridine) were first demonstrated by Murray and co-workers [7–11] and others [12–14] in the early 1980s. Extensive literature is now available on these and other related materials [15, 16]. Such studies have conclusively demonstrated that transition metal complexes containing vpy undergo electroreductively onset polymerization, responsible for deposition of electroactive films of the corresponding monomer complex. In an electroreductive process, films are generated in the cathodic region of the substrate, yielding protective action to the steel and granting better stability upon polymerization. We have demonstrated that this class of monomers acts efficiently in the electrodeposition of adherent films onto Pt, Pd, and sintered Fe(5–10)%-Ni electrodes [6]. In addition to the protective nature of the polymeric coat, the presence of ruthenium in the film plays an important role in the system, since Ru^{2+} can be oxidized to Ru^{3+} and reduced back to its original valence state. Reversible anodic sites can then be formed in the film, keeping the substrate from oxidizing. Coating stainless steel with such polymeric films improves the protective action to chloride environments, preventing localized pitting corrosion during transport and storage.

The present study discusses preliminary data on the corrosion resistance of both bare and coated 17-4 PH sintered steel. Scanning electron microscopy (SEM) was used to observe the morphology of the coating layers, to estimate their thickness, and to assess the general aspect of corroded specimens. Elementary energy dispersive spectroscopy (EDS) analysis was carried out to estimate the composition of the coating layer. Cyclic voltammetry tests were also performed to observe the electrochemical behavior of the films. Finally, the corrosion resistance of the system was studied by anodic polarization.

Experimental

Solutions and chemicals

The synthesis of {*trans*-[RuCl$_2$(vpy)$_4$]} has been described elsewhere [6]. Commercially available chemicals and solvents of an analytical grade were used in the synthesis of the monomer. The main products employed were 4-vinylpyridine (Aldrich), trihydrated ruthenium chloride (Jonhson Matthey), and solvents (Grupo Química). Chromatographic grade solvents were employed in the electrochemical analyses. The electrodeposition solution consisted of 3×10^{-3} M {*trans*-[RuCl$_2$(vpy)$_4$]} (monomer) and 0.1 M tetrabutylammonium hexafluorophosphate (TBAF, Aldrich) dissolved in acetonitrile/dichloromethane (4:1). The solution used in the anodic polarization curves consisted of 3% sodium chloride (Grupo Química). TBAF (0.38 g) dissolved in methyl isobutyl ketone (10 mL) was used as the electrolyte solution to study the electrochemical behavior of the coated steel electrodes.

Techniques and electrodes

Electrodeposition and electrochemical tests were carried out using a potentiostat/galvanostat (EG&G PAR, model 283) connected to a Pentium computer using a GPIB IEEE 488 interface board. The polarization plots were conducted with softcorr III (corrosion measurement software for Windows) computer program (EG&G).

A pseudo reference consisting of a platinum sheet (size: 0.1 cm thickness, 0.7 cm width, 2.0 cm length; exposed area to the solution: 2.1 cm^2) placed at a distance of 0.5 cm from the working electrode was used during the electrodeposition experiments (in 0.1 M TBAF dissolved in acetonitrile/dichloromethane 4:1) and cyclic voltammetry experiments (in 0.38 g TBAF dissolved in 10 mL methyl isobutyl ketone). In addition, an Ag/AgCl reference electrode was used in the anodic polarization experiments (in 3% NaCl). The counter electrode used was a platinum sheet (size: 0.1 cm thickness, 0.7 cm width, 2.0 cm length; exposed area to the solution: 2.1 cm^2). The working electrode employed was a 17-4 PH stainless steel injection molded specimen (size: 0.3 cm thickness, 0.9 cm width, 4.2 cm length; exposed area: 2.1 cm^2 to the electrodeposition solution, 0.25 cm^2 to the cyclic voltammetry experiments and 0.95 cm^2 to the anodic polarization experiments). The composition of the injected 17-4 PH steel was analyzed by X-ray fluorescence (XRF), yielding: Cr 18.10 wt%, Ni 8.50 wt%, Mn 0.70 wt%, Si 0.93 wt% and Mo 2.10 wt%. Powdered steel samples were injected and sintered by the Steelinject Division of Lupatech (Caxias do Sul, Brazil). The main process parameters employed are summarized as: pre-sintering profile: 980 °C/1 h; pre-sintering atmosphere: H$_2$; sintering profile: 1350 °C/3 h; sintering atmosphere: vacuum, Ar, H$_2$; final density: 7.61 g/cm^3.

Prior to electrodeposition, the steel samples were surface ground using 220–600 sandpaper and polished in an alumina slurry ($\phi = 0.3$ μm to $\phi = 0.25$ μm) in order to obtain a good finish. The samples were then immersed in a carbon tetrachloride ultrasonic bath for 5 min. Poly{*trans*-[RuCl$_2$(vpy)$_4$]} films were potentiostatically grown onto 17-4 PH stainless steel at an applied potential of −2.75 V during 54 min. In Fig. 1 is shown the electrodeposition curve of poly{*trans*-[RuCl$_2$(vpy)$_4$]} deposited potentiostatically on 17-4 PH steel. The charge density that follows from the integration of the I/t curve was evaluated as 1.4 C/cm^2. This value covers a process that probably includes the electropolymerization itself and secondary processes such as degradation of the axial ligands and oxygen reduction (dissolved in the solution). Thus, the real charge involving only the polymerization reaction and consequently the m_e (electrochemical equivalent) could only be available with a knowledge of the polymerization mechanisms of poly{*trans*-[RuCl$_2$(vpy)$_4$]}, which are not completely elucidated in the literature at present.

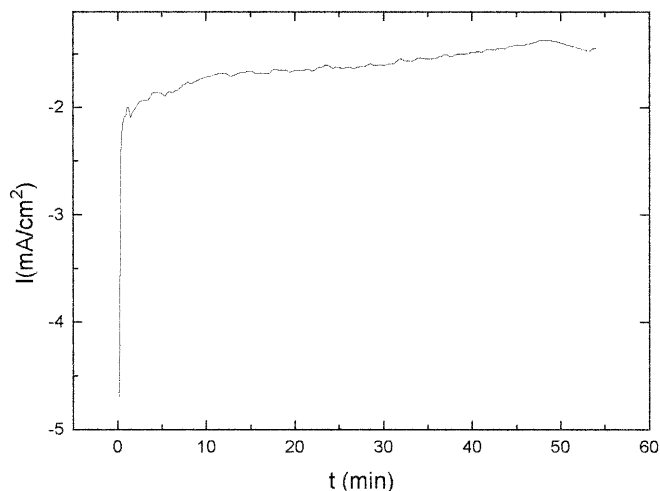**Fig. 1** Potentiostatic curve of the cathodic film-forming electrodeposition of poly{*trans*-[RuCl$_2$(vpy)$_4$]} on 17-4 PH stainless steel at −2.75 V during 54 min

Adherence tests

The adherence of electrodeposited polymeric layers on 17-4 PH steel substrates was estimated by a standard peeling test [17]. This method evaluates the adherence and flexibility of paint coatings on substrates. Each test was performed for three samples coated under the same conditions. The samples were cut in six parallel (horizontal) lines at a distance of 1 mm from each other, and six parallel (vertical) lines in order to obtain a grid of 25 squares. An adhesive (2721, Scotch 3 M) was applied to the grid and then, detached. After that, the film was compared with a standard grid, as shown in Table 1.

Polarization curves

The polymeric films were also characterized according to the corrosion rate. Related parameters such as active region, passive region, and transpassivation were also determined from anodic polarization plots. The experimental conditions are displayed in Table 2. The initial potential was set to −250 mV vs. OCP (open circuit potential) at a scanning rate of 0.8 mV/s.

Cyclic voltammetry

Cyclic voltammetry was employed to observe the electrochemical behavior of 17-4 PH steel samples coated by poly{*trans*-[RuCl$_2$(vpy)$_4$]}. The experiments were carried out for scanning rates ranging from 0.4 to 2.0 mV/s.

Table 1 Standard grid used in the adherence pull-off test [18]

Code	Description	Figure
GR0	nothing detached from the sample	–
GR1	5% detached from the sample	
GR2	15% detached from the sample	
GR3	35% detached from the sample	
GR4	65% or more detached from the sample	

Table 2 Electrochemical parameters measured from the voltammograms obtained for 17-4 PH steel samples coated by poly{*trans*-[RuCl$_2$(vpy)$_4$]} (Fig. 5)

Curve	Scanning rate (mV/s)	E_{pa} (mV)	E_{pc} (mV)	ΔE (mV)	$E_{1/2}$ (mV)	I_{pa} (μA/cm^2)	I_{pc} (μA/cm^2)	I_{pc}/I_{pa}
A	0.4	158	88	70	123	7	−12	−1.7
B	0.6	133	67	66	100	6	−8	−1.3
C	0.8	110	38	73	74	3.5	−6	−1.7
D	1.0	112	−1	111	55	3.4	−5	−1.5
E	1.5	109	−4	114	52	3.4	−4.8	−1.4
F	2.0	103	−12	116	45	3.4	−4.7	−1.4

Morphological characterization and elementary analysis

The polymeric films were analyzed by a Philips XL-30 scanning electron microscope equipped with an energy dispersive spectrometer. Morphology, thickness, and composition of the films were investigated.

Corrosion tests: salt spray tests were performed with the 17-4 PH stainless steel specimens during 30 days. Acid rain simulated tests were conducted with 17-4 PH stainless steel specimens during 120 days. Both tests were performed following the technical specification [18].

Results and discussion

Morphological characterization, elementary analysis and adherence tests

Mechanically dislodging poly{*trans*-[RuCl$_2$(vpy)$_4$]} films from the surface of electrodes usually consists of a laborious process. Thus, SEM studies were performed on coated steel surfaces with no need for gold sputtering. Charging was prevented by the improved conductivity of the film itself. Figure 2 illustrates some morphological aspects of a cross-section of a polymeric film deposited on 17-4 PH stainless steel. The film is approximately 100 μm thick, and essentially uniform, depicting a reddish opaque hue. It could also be noticed that the film penetrated into open pores, coating an additional area exposed to corrosive attack. The influence of porosity on the corrosiveness of sintered steel has been extensively documented by previous literature reports [19–22]. A similar scenario has been observed for sintered Fe-1.5%Si and Fe-1.5%Mo steel [22], where the corrosion resistance of the alloy can be considerably reduced by the inherent presence of residual open porosity. In addition, other studies concerning the corrosion resistance of stainless steel reported that excessive open porosity increased the exposed area to the corrosive environment. This induces crevice corrosion [23], with the formation of concentration cells in the pores [24, 25]. Otero et al. [26] have provided further confirmation of this fact upon studying 316L and 304L steels in organic acids. The successful coating of open pores by poly{*trans*-[RuCl$_2$(vpy)$_4$]} (Fig. 2) is an important aspect in driving further research towards improving corrosion protection of sintered steels.

Results from an EDS analysis carried out for a 17-4 PH stainless steel specimen coated by poly{*trans*-

Fig. 2 Scanning electron micrograph of a cross section of poly{*trans*-[RuCl$_2$(vpy)$_4$]} film deposited potentiostatically ($E = -2.75$ V$_{Ag/Ag^+}$) during 54 min on the 17-4 PH stainless steel substrate. Magnification: 200

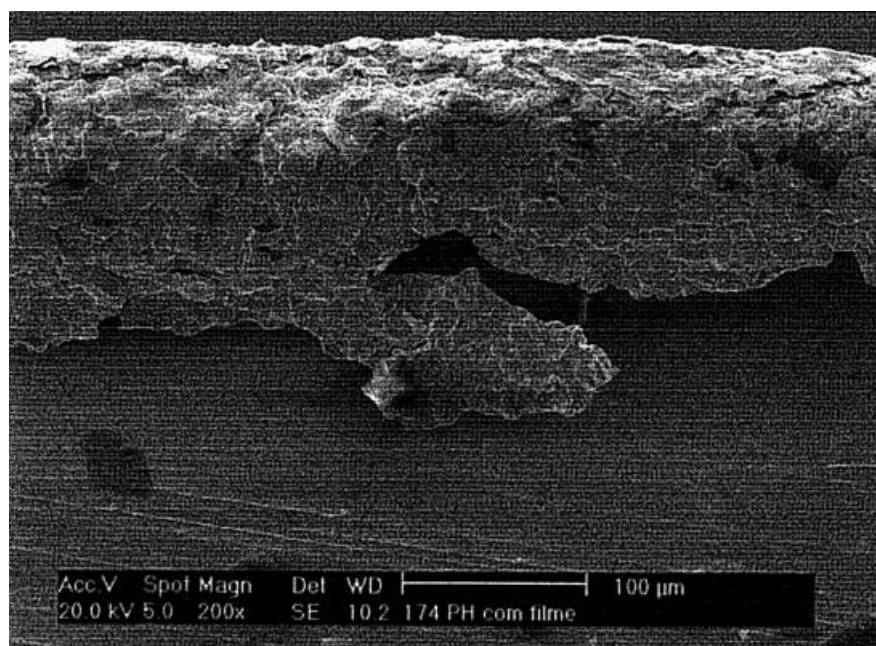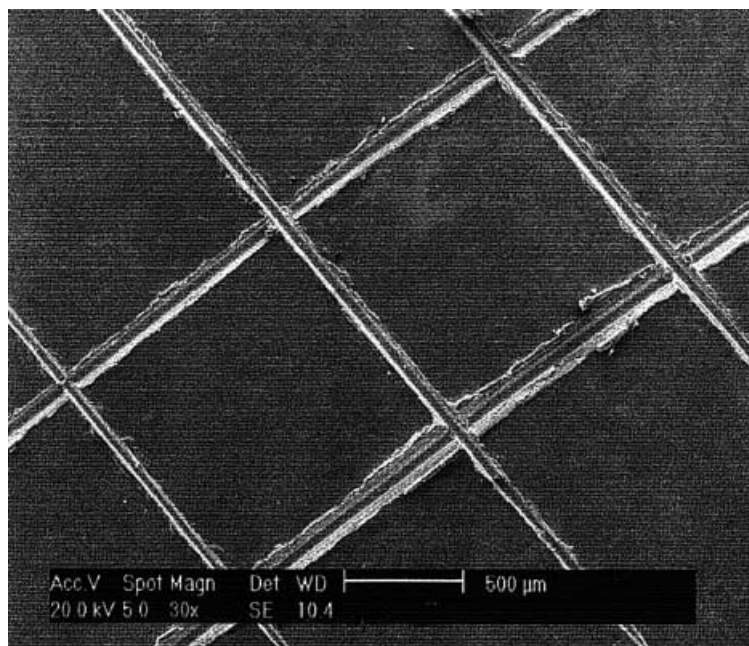[RuCl$_2$(vpy)$_4$] indicated the presence of ruthenium in the film. Chlorine and carbon lines corresponding to the axial vpy and Cl$^-$ ligands, coordinated in ruthenium complexes, could also be observed. Relatively wide peaks related to alloying elements were also observed and suggested the presence of a large number of pores and defects in the film structure.

The results of the adherence tests carried out for poly{*trans*-[RuCl$_2$(vpy)$_4$]} films suggested nearly full adherence to the metallic substrate for every specimen analyzed, as can be seen in Fig. 3.

Electrochemical characterization: cyclic voltammetry

Voltammograms corresponding to steel samples were compared with those obtained on platinum substrates coated with a polymeric film obtained in TBAF/methyl isobutyl ketone medium at a scanning rate of 0.8 mV/s (Fig. 4). Curves A (polymeric coating on platinum) and B (polymeric coating on steel) clearly show the presence of two well-defined peaks related to the Ru^{2+}/Ru^{3+} redox reaction. This result confirms literature data obtained for the same complex deposited on a platinum specimen [6]. In curve A, the anodic peak shows the maximum potential value (E_{pa}) at approximately −96 mV, whereas the cathodic peak (E_{pc}) is at −140 mV. A corresponding ΔE value of 43 mV is then obtained. On the other hand, E_{pa} for curve B is at +110 mV and E_{pc} at +38 mV. In this case, ΔE comes to 72 mV. Preliminary results reported in the literature [6] indicated that, in contrast to those observed for 17-4 PH stainless steel coated specimens, peaks related to the Ru^{2+}/Ru^{3+} process on polymeric coated platinum sheets were reversible.

Figure 5 shows cyclic voltammograms obtained for a polymeric coated 17-4 PH stainless steel substrate. The
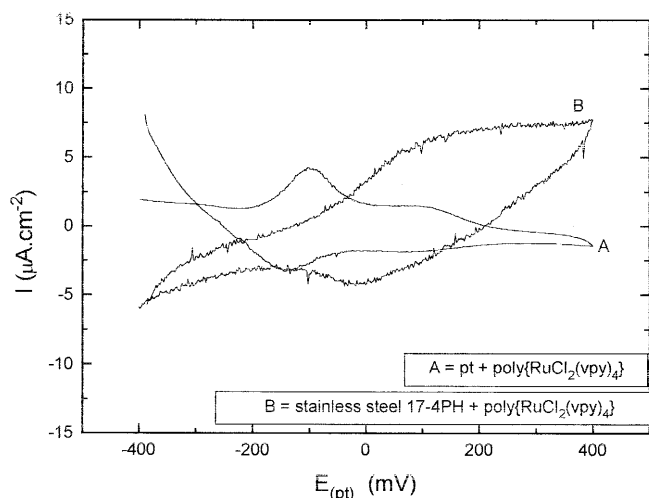

Fig. 4 Voltammetric curves for 17-4 PH steel and platinum samples coated by a poly{*trans*-[RuCl$_2$(vpy)$_4$]} in 0.1 M TBAF/methyl isobutyl ketone medium. Scanning rate: 0.8 mV/s

associated current plot exhibits a characteristic diffusional tail at the peak base, as well as peak asymmetry. Such features imply that diffusional transport within the film is the rate-limiting factor. This type of response can be observed in thick films and further confirms the observed values for the film thickness. Figure 5 depicts some singular characteristics concerning the electrochemical behavior of polymeric films on substrates. The main difference observed, compared to similar complexes deposited on platinum or palladium substrates, involves the scanning rates used to perform the electrochemical experiments. For Pt or Pd substrates, scanning rates of 50–500 mV/s are usual [6]. It was observed in the present study that such scanning rates are quite high for 17-4 PH
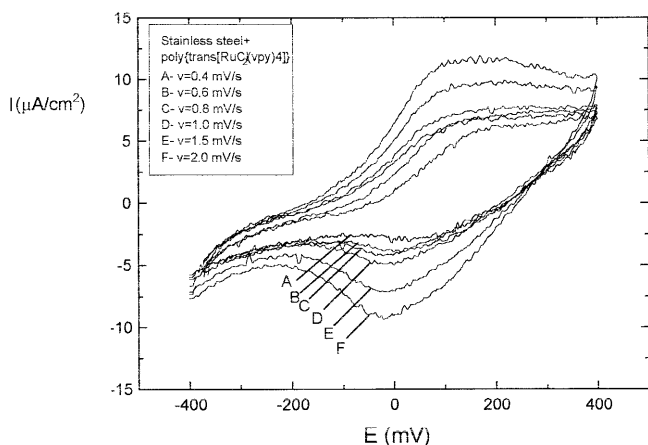
Fig. 5 Voltammetric curves for 17-4 PH steel samples coated by poly{*trans*-[RuCl₂(vpy)₄]} in 0.1 M TBAF methyl isobutyl ketone medium, at different scanning rates

Fig. 6 Plot of I_p vs. scan rate corresponding to the film depicted in Fig. 5

stainless steel specimens. Thus, it was not possible to clearly identify the main peaks related to the redox reaction of the metal center (Ru) nor to the axial ligands of the polymeric complex at the same scanning rates usually used for Pt sheets. Therefore, the scanning rates had to be reduced to values within the 0.4–2.0 mV/s range. The calculated current densities (Table 2) were in the range of 3–12 µA/cm² and demonstrated that the polymeric films obtained on steel samples were less electroactive than those deposited on Pt.

In curve A (0.4 mV/s), the redox process is metal-centered, with $E_{pa} = 158$ mV attributed to the *trans*-[RuCl₂(vpy)₄]$^{0/+}$ process. The reverse wave, observed at 88 mV, corresponded to the *trans*-[RuCl₂(vpy)₄]$^{+/0}$ process. This leads to an $E_{1/2}$ value of 123 mV vs. the pseudo Pt reference. It was observed that E_{pa} values shifted from 158 to 103 mV and E_{pc} from 88 to −12 mV, as the scanning rate increased from 0.4 to 2.0 mV/s. As a consequence, $E_{1/2}$ values decreased from 123 to 45 mV with increasing scanning rates. These values differ slightly from those reported by Franco and co-workers [6] for the same complex deposited on platinum substrates.

With respect to the degree of reversibility observed for poly{*trans*-[RuCl₂(vpy)₄]} films electrodeposited on 17-4 PH stainless steel substrates, they all depicted both oxidation and reduction peaks characteristic of the Ru²⁺/Ru³⁺ redox reaction. In addition, the reversible features disappeared by either increasing the scanning rate or the number of cycles. This indicates that the electrical conductivity of the films decreased during the electrochemical experiments. Voltammetric plots of thick electrochemically coated layers also show typical behavior suggesting charge and discharge of a capacitor, noticeably a high double-layer capacitance at potentials higher than that of the redox couple of ruthenium. The variation of peak current with the sweep rate is also diagnostic. A series of cyclic voltammograms, obtained at various scan rates, surprisingly showed a change from $v^{1/2}$ behavior to a scan rate
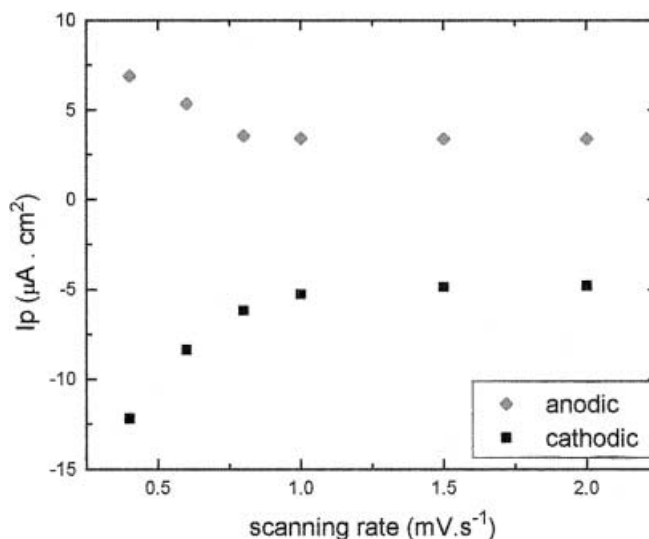
independent plot, as the sweeping rate increased (Fig. 6). Such a change in behavior is probably determined by the interdependent relationship between the sweeping rate and the kinetics of the voltammetric behavior throughout the film.

Table 2 indicates that the I_{pc}/I_{pa} ratio departs from unity at the entire scan rate investigated. Consecutive scans around the redox couple showed that the voltammetric profiles tend to reduce the measured current densities as the number of cycles increase. Similar behavior was not observed for poly{*trans*-[RuCl₂(vpy)₄]} films deposited on a platinum substrate [6], where the polymeric films showed good stability of the complex in solution. The integrated voltammetric charge recorded under the current peak can be used to estimate the apparent surface coverage Γ_{APP} of immobilized electroactive species in the polymeric film. These estimates were calculated for slow sweep rates, in order to assure long times for the redox reactions, and hence a greater number of transformed redox sites along the film. For a scan rate of 0.4 mV/s, the integrated charge totaled 1.3×10^{-9} µC/cm², whereas the apparent surface coverage came to $\Gamma = 1.4879 \times 10^{-8}$ mol/cm², according to:

$$\Gamma = \frac{Q}{nF}$$

where Q is the integrated charge under the voltammetric peak. This result can be rationalized considering the value of Γ obtained from integration of the voltammetric waves, calculated to be 2.50×10^{-8} mol/cm² for electrocoated *trans*-[RuCl₂(vpy)₄] on platinum electrodes [6]. This number corresponds to approximately 300 monolayers, according to the model proposed in the literature [27], which gives 8.3×10^{-11} mol/cm² for a monolayer.

The full peak width at half height (FWHH) in the voltammetric wave (Table 3) conveys useful information

on the electrochemistry of redox switching within poly{*trans*-[RuCl$_2$(vpy)$_4$]} films. Assuming an ideal situation characterized by no interredox center interaction, and an equilibrium of the sites in the layer for a potential applied at the support electrode surface, the FWHH yields $(90.6/n)$ mV at $T = 198$ K [28]. Data shown in Table 3 include FWHH values that exceed this ideal limit, which confirms reports [29–31] that FWHH values are typically higher than estimated. In layers formed by immobilized redox centers, sensitive variations in the structure, solvation, and environment can occur. Such modifications result in complex spectra of redox sites with closely spaced but distinct standard potentials or activity effects. Occupied redox sites may show repulsive interactions, which ultimately promote alternating site occupancies, thus broadening the voltammetric peak response [32].

Polarization curves

Anodic polarization curves obtained for both bare and coated 17-4 PH steel substrates in 3% NaCl are shown in Fig. 7. The corresponding electrochemical parameters are summarized in Table 4. The associated corrosion potential of the uncoated sample (curve A) was -30 mV$_{Ag/Ag}{}^+$. The coated sample (curve B) had a corrosion potential of -300 mV$_{Ag/Ag}{}^+$. In curve A it can be observed that the dissolution of the substrate takes place at 300 mV$_{Ag/Ag}{}^+$, shifting the curve to anodic regions. In curve B, a peak corresponding to the Ru^{2+}/Ru^{3+} redox reaction can also be observed. The calculated peak area gives a charge density of 7.353 μC/cm^2. According to Coulomb's law, it is possible to estimate the concentration of ruthenium in the polymeric film: 7.64×10^{-5} mol/cm^2, which corresponds to 45.9929×10^{18} molecules of *trans*-{RuCl$_2$(vpy)$_4$ per cm^2. The morphology of the coating films remained unaffected after the polarization tests in 3% NaCl. In addition,

significant mass changes were not observed in the coated samples after these tests. This indicates a good performance of the coat in chloride environments. Further electrochemical corrosion tests (EIS) are presently under way to evaluate the efficiency of those films in several aggressive environments.

Corrosion tests

It was observed in the salt spray tests by visual inspection that the coated 17-4 PH stainless steel resisted corrosive attack during the whole experiment. However, these samples did not resist an acid rain environment during the first 2 days of exposure, probably because of corrosive attack by H$^+$ species.
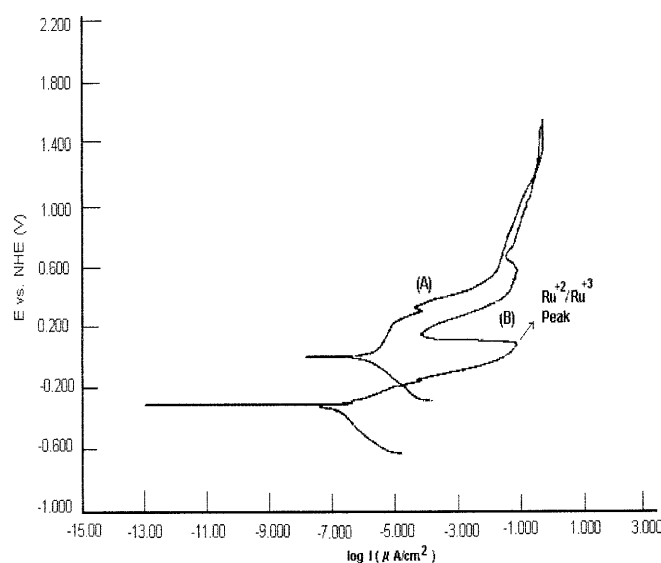

Fig. 7 Polarization curves of 17-4 PH steel (*A*) and 17-4 PH steel coated by poly{*trans*-[RuCl$_2$(vpy)$_4$]} (*B*) in 3% NaCl medium, at a scanning rate of 0.8 mV/s

Table 3 Electrochemical parameters measured from the voltammograms obtained for 17-4 PH steel samples coated by poly{*trans*-[RuCl$_2$(vpy)$_4$]} (Fig. 5)

Curve	Scanning rate (mV/s)	Q_a (μC/cm^2)	Q_c (μC/cm^2)	Q_c/Q_a	FWHM anodic	FWHM cathodic
A	0.4	1435.95	4027.34	2.80	221.83	377.01
B	0.6	1411.84	3226.58	2.28	223.03	406.13
C	0.8	1017.67	2652.38	2.60	266.55	436.45
D	1.0	1049.87	2371.17	2.26	274.96	443.65
E	1.5	1019.46	2141.35	2.10	276.46	445.43
F	2.0	916.11	1771.04	1.93	278.86	551.11

Table 4 Electrochemical parameters measured from the anodic polarization curves obtained for 17-4 PH steel samples and for 17-4 PH steel samples coated by poly{*trans*-[RuCl$_2$(vpy)$_4$]} (measured at $E = 0.25$ V from Fig. 7). *mpy* Millimeters per year

Sample	$E_{I\,=\,0}$ (mV)	β_a (V/decade)	β_c (V/decade)	I_{corr} (μA/cm^2)	Corrosion rate (mpy)
17-4 PH	29	0.328	0.172	1.286	0.509
17-4 PH coated with poly{*trans*-[RuCl$_2$(vpy)$_4$]}	301	0.060	0.172	0.087	0.035

Conclusions

The results gathered herein demonstrate that the *trans*-$[RuCl_2(vpy)_4]$ monomer can be electrodeposited on the surface of 17-4 PH steels using potential-controlled techniques. EDX analyses of poly{*trans*-$[RuCl_2(vpy)_4]$} coated 17-4 PH steel revealed the presence of a ruthenium redox center, in addition to chlorine and carbon, corresponding to axial ligands of the complex. SEM imaging showed that poly{*trans*-$[RuCl_2(vpy)_4]$} films are essentially uniform and approximately 100 µm thick. The coating layers tended to penetrate into the open pores of the substrate. Cyclic voltammograms indicated that similar polymeric films deposited on platinum sheets showed higher reversibility than those produced on steel substrates. Coated 17-4 PH steel substrates were not subjected to corrosive action.

References

1. (a) Mengoli G, Munari MT, Bianco P (1981) J Appl Polym Sci 26: 4247; (b) Troch-Nagels RG, Winand A, Weymeersch LR (1992) J Appl Electrochem 22: 756; (c) Sitaram SP, Stoffer JO, O'Keefe TJ (1997) J Coat Technol 69: 65
2. (a) Beck F (1988) Electrochim Acta 33: 839; (b) Tallman DE, Pae Y, Chen G, Bierwagen GP, Reems B, Gelling VJ (1998) Annn Tech Conf – Soc Mast Eng 56: 1234–1237
3. Paula MMS, Franco CV (1996) J Coord Chem 40: 71
4. Franco CV, Prates PB, de Moraes VN Jr, Paula MMS (1997) Synth Met 90: 81
5. Bandeira MCE, Franco CV, Martini E (1999) J Solid State Electrochem 3: 210
6. Paula MMS, de Moraes VN, Mocellin F, Franco CV (1998) J Mater Chem 8: 2049
7. Jernigan JC, Wilbourn KO, Murray RW (1987) J Electroanal Chem 222: 193
8. Wilbourn KO, Murray RW (1998) J Phys Chem 92: 3642
9. Coury LA Jr, Oliver BN, Egekeze JO, Sosnoff CS, Brumfield JC, Buck RP, Murray RW (1990) Anal Chem 62: 452
10. Pickup PG, Kutner W, Leidner CR, Murray RW (1984) J Am Chem Soc 106: 1991
11. Denisevich P, Abruña HD, Leidner CR, Meyer TJ, Murray RW (1982) Inorg Chem 21: 2153
12. Belanger D, Wrighton MS (1987) Anal Chem 59: 1426
13. Goldsby KA, Meyer TJ (1984) Inorg Chem 23: 3002
14. Lyons MEG (1994) Electroactive polymer electrochemistry, part 1. Plenum Press, New York, pp 6–7
15. Guarr TF, Anson FC (1987) J Phys Chem 91: 4037
16. Elliot CM, Baldy CJ, Nuwaysir LM, Wilkins CL (1990) Inorg Chem 29: 389
17. ASTM (1980) ASTM D 870-54. American Society for Testing Materials, Philadelphia
18. ASTM (1994) ASTM B 117-94. American Society for Testing Materials, Philadelphia
19. Borges PC, Pereira NC, Franco CV, Klein AN (1994) Adv Powder Metall Particulate Mater 2: 61
20. Sobral AVC, Maliska AM, Tosi G, Muzart JLR, Klein AN, Franco CV (1995) Adv Powder Metall Particulate Mater 3: 11
21. Pereira NC, Mittelstadt FG, Spinelli A, Franco CV, Maliska AM, Klein AN, Muzart JLR (1995) J Mater Sci 30: 4817
22. Sobral AVC, Boblitz Parente AC, Muzart JLR, Franco CV (1997) Surf Coat Technol 92: 10
23. Mathiesen T, Maahn E (1995) Adv Powder Metall Particulate Mater 3: 45
24. Fedrizzi L, Deflorian F, Tiziani A, Cristofolini I, Molinari A (1994) Adv Powder Metall Particulate Mater 7: 273
25. Tremblay A, Angers R (1995) Adv Powder Metall Particulate Mater 7: 225
26. Otero E, Pardo A, Utrilla MV, Pérez FJ, Merino C (1997) Corros Sci 39: 453
27. Kalir R, Zilkha A (1978) Eur Polym J 14: 557
28. Lyons MEG (1994) Electroactive polymer electrochemistry, part 1. Plenum Press, New York, pp 84–147
29. Laviron E (1979) J Electroanal Chem 100: 263
30. Smith DF, Willman K, Kuo K, Murray RW (1979) J Electroanal Chem 95: 217
31. Lennox JC, Murray RW (1978) J Am Chem Soc 100: 3710
32. Murray RW (1992) In: Murray RW (ed) Molecular design of electrode surfaces. (Techniques of chemistry series, vol 22). Wiley-Interscience, New York, pp 1–48